Research article

Journal of RAMAN SPECTROSCOPY

Received: 27 April 2016 Accepted: 21 May 2016 Published online in Wiley Online Library: 28 June 2016

(wileyonlinelibrary.com) DOI 10.1002/jrs.4967

Phase-specific Raman analysis of *n*-alkane melting by moving-window two-dimensional correlation spectroscopy

Ying Jin,[a] Anthony P. Kotula,[b] Angela R. Hight Walker,[c] Kalman B. Migler[b] and Young Jong Lee[a]*

We use moving-window two-dimensional correlation spectroscopy (MW-2DCOS) for phase-specific Raman analysis of the *n*-alkane ($C_{21}H_{44}$) during melting from the crystalline solid phase to the intermediate rotator phase and to the amorphous molten phase. In MW-2DCOS, individual peak-to-peak correlation analysis within a small subset of spectra provides both temperature-resolved and spectrally disentangled Raman assignments conducive to understanding phase-specific molecular interactions and chain configurations. We demonstrate that autocorrelation MW-2DCOS can determine the phase transition temperatures with a higher resolving power than commonly used analysis methods including individual peak intensity analysis or principal component analysis. Besides the enhanced temperature resolving power, we demonstrate that asynchronous 2DCOS near the orthorhombic-to-rotator transition temperature can spectrally resolve the two overlapping peaks embedded in the Raman CH_2 twisting band in the orthorhombic phase, which had been only predicted but not observed because of thermal broadening near the melting temperature. Published 2016. This article is a U.S. Government work and is in the public domain in the USA.

Additional supporting information may be found in the online version of this article at the publisher's web site.

Keywords: Raman spectroscopy; moving window; two-dimensional correlation spectroscopy; *n*-alkane; phase transition

Introduction

Understanding temperature-dependent structures of saturated linear hydrocarbons or *n*-alkanes is important for improving their petrochemical applications for oils, lubricants, and fuels, and for elucidating the hierarchical morphology of more complex materials, such as polyethylene (PE) and lipid bilayers.[1,2] In general, long carbon chain alkanes have an orthorhombic crystalline phase below the melting temperature and a randomly oriented amorphous phase above the melting temperature. Interestingly, previous X-ray and Raman studies show that some *n*-alkanes ($20 \leq n \leq 37$) can have mobile intermediate phases between the crystalline phase and the amorphous phase.[3,4] The intermediate phases are called rotator phases, where predominantly *trans* chains can rotate along the chain axis and are packed in the hexagonal lattice with long range order.[5]

Raman spectroscopy is widely used to characterize the phases of *n*-alkanes and PE by measuring vibration frequencies affected by short-range interchain interactions and chain conformations (*trans vs gauche*). Raman bands of the amorphous phase are characterized by relatively broad bandwidths because of disordered chain conformation and high *gauche* concentration. On the other hand, both the orthorhombic crystalline phase and the rotator phases are rich in *trans* conformation, together called the consecutive *trans* phase,[6] exhibiting relatively narrow Raman bandwidths. At the molecular length scale, the crystalline phase supports two different types of interchain interactions in the orthorhombic unit cell while the rotator phases have only one type in the hexagonal unit cell. The two types of interchain interactions in the orthorhombic phase can cause splitting in some Raman bands. For example, the CH_2 bending mode appears as a single peak at 1438 cm^{-1} in the rotator phase but becomes split in the orthorhombic phase as much as by 25 cm^{-1}.[7] One of the split peaks, at 1417 cm^{-1}, is used as a metric to determine the mass fraction of the orthorhombic conformation.[7,8] For most other Raman bands, however, the crystal-field splitting in the orthorhombic phase is smaller than the Raman bandwidth at room temperature; therefore, the peak splitting has been observed only at extreme conditions, such as at liquid nitrogen temperature[9,10] or from single crystals.[11] Such subtle spectral changes are challenging for conventional fitting-based individual peak analysis to decipher. In this work, we demonstrate that moving-window two-dimensional correlation spectroscopy (MW-2DCOS) analysis can unravel peak splitting from temperature-dependent Raman spectra measured near the melting temperature.

* *Correspondence to: Young Jong Lee, Biosystems and Biomaterials Division, National Institute of Standards and Technology, Gaithersburg, MD 20899, USA. E-mail: youngjong.lee@nist.gov*

The authors declare no competing financial interest.

a *Biosystems and Biomaterials Division, National Institute of Standards and Technology, Gaithersburg, MD, 20899, USA*

b *Materials Science and Engineering Division, National Institute of Standards and Technology, Gaithersburg, MD, 20899, USA*

c *Physical Measurement Laboratory, National Institute of Standards and Technology, Gaithersburg, MD, 20899, USA*

The 2DCOS method is a versatile, qualitative analysis tool that has been used to analyze the effect of a perturbation, such as temperature, pressure, concentration, pH, and time, on the spectral response.[12] 2DCOS is based on pair-wise (*bivariate*) analysis, which can be compared with *univariate* individual peak analysis and *multivariate* analysis (MVA). The individual peak analysis can provide more intuitive links between spectral changes and perturbation but is very limited in sensitivity specifically in crowded spectral regions. On the other hand, MVA, which considers intensity variation of a large number of spectral components, is able to detect and quantify spectral changes as a function of perturbation. However, MVA is limited in providing direct correlation of individual peaks with the variable perturbation. 2DCOS provides both direct spectral correlation with specific perturbation and resolving power to detect subtle spectral changes and overlapping peaks. Additionally, the in-phase and out-of-phase correlation spectral maps generated by 2DCOS elucidate the direction and sequence of spectral changes between pairs of spectral components over a perturbation range.[13,14] In some cases, spectral changes occur over a narrow perturbation range; thus, it may be more useful to limit 2DCOS to this specific range in order to identify the relevant spectral features, which can be examined by moving-window 2DCOS (MW-2DCOS). In the MW-2DCOS analysis, a small subset or window of spectra is scanned over the whole perturbation range while analyzed by 2DCOS. This MW-2DCOS method has been previously demonstrated to determine phase transition temperature and the associated spectral features.[15–18]

In this paper, we analyze a series of temperature-dependent Raman spectra of melting *n*-$C_{21}H_{44}$. We use various methods to analyze the data including fitting-based peak intensities, principal component analysis, simple 2DCOS over a wide temperature range, and MW-2DCOS with a narrow temperature window. We demonstrate that the autocorrelation spectra of MW-2DCOS can determine the transition temperatures (orthorhombic-to-rotator and rotator-to-amorphous) with the highest resolving power among the demonstrated analysis methods. Temperature dependences of peak positions and widths of several Raman bands confirm that the intermediate, rotator phase influences the Raman modes differently from the crystalline and the amorphous phases. Furthermore, our comparative analysis of asynchronous correlation maps of the CH_2 twisting mode indicates that the consecutive *trans* Raman band exists as two overlapping peaks in the orthorhombic phase but as a single peak in the rotator phase.

Experimental section

Sample preparation

Heneicosane (*n*-$C_{21}H_{44}$) was purchased from Sigma Aldrich (≥99.5%) and used without purification. The original alkane flakes were broken into smaller pieces in order to generate a homogeneous scattering volume for Raman measurement and then loaded into a shear cell (Linkam Scientific Instruments, CSS 450) with quartz disks. The sample was compressed into a thickness of 1 mm. The shear cell provided optical access to the sample at a controlled temperature.

Raman spectroscopy

Raman spectra were measured with a triple grating Raman spectrometer (Horiba, T64000; spectral resolution = 0.8 cm^{-1}) in the 180° backscattering geometry. Lineally polarized light from a HeNe laser (632.8 nm) was focused into a spot with an approximately 60-μm diameter, and an average power of 15 mW. The sample was heated from 28 °C to 45 °C. Three consecutive Raman spectra were recorded and averaged at each temperature 2 min after the sample was equilibrated. It took approximately 3 min to acquire each spectrum for a scanning range of 950 cm^{-1} to 1550 cm^{-1}, and 9 min for three spectra at each temperature. Between 30 °C and 42 °C, Raman spectra were measured with an increment of 1 °C. Raman spectra at 28 °C and 45 °C were found to be indistinguishable from those at 30 °C and 42 °C, respectively; therefore, when needed for MW-2DCOS, Raman spectra at 29 °C, 43 °C, and 44 °C were generated by interpolation with the neighboring, almost identical spectra. All spectra were detrended by a splined baseline subtraction method with zeros at four frequencies (950 cm^{-1}, 1240 cm^{-1}, 1350 cm^{-1}, and 1550 cm^{-1}). To compensate irregular scattering, the baseline-detrended spectra were normalized by the area of the CH_2 twisting band (1240 cm^{-1} to 1350 cm^{-1}).[7,8]

Principle component analysis (PCA)

PCA was performed with a commercial multivariate analysis package (Solo + MIA, Eigenvector Research, Inc). The intensity-scaled Raman spectra were mean-centered before performing PCA.

Two-dimensional correlation spectroscopy (2DCOS)

All 2DCOS analyses, including MW-2DCOS, were performed with the "2D Shige" software, which was developed by Shigeaki Morita (Kwansei Gakuin University).

Results and discussion

Figure 1a shows selected Raman spectra acquired from *n*-$C_{21}H_{44}$ while it was heated from 28 °C to 45 °C. Migler *et al.*[8] analyzed peak intensities of several Raman bands representing the orthorhombic, consecutive *trans*, and amorphous phases of alkane and PE by fitting with Lorentzian functions. Similarly, Fig. 1b shows plots of the integrated area of the fitted peaks centered at 1417 cm^{-1}, 1295 cm^{-1}, and 1300 cm^{-1}. The 1417 cm^{-1} peak results from the crystal field splitting of the CH_2 bending mode only in the orthorhombic crystalline phase and disappears in the rotator phase. The CH_2 twisting mode exists as a narrow peak at 1295 cm^{-1} in the consecutive *trans* conformation (from the orthorhombic and rotator phases) and becomes a broad peak at 1300 cm^{-1} in the amorphous phase. Later in the paper, we discuss fitting results of the consecutive *trans* peak at 1295 cm^{-1} with a pseudo-Voigt function, which does not change the peak intensity plot shown in Fig. 1b. In Fig. 1b, the consecutive *trans* peak decreases very gradually as the amorphous peak at 1301 cm^{-1} increases from 34 °C to 42 °C. In contrast, the orthorhombic peak at 1417 cm^{-1} disappears sharply at 33 °C, exhibiting a sharp transition from the orthorhombic crystalline phase into the rotator phase.[8] This type of individual peak intensity analysis can provide explicit information of phase transitions when distinctive bands can be unambiguously associated with each phase. However, when bands are embedded in spectrally crowded regions, individual peak intensities become unreliable because of difficulty in separating the relative contributions of neighboring peaks. Also, for complex systems where multiple molecular conformations coexist, such as PE, it is not trivial to track subtle spectral changes of individual bands by fitting the overlapping peaks during phase transitions.

Journal of RAMAN SPECTROSCOPY

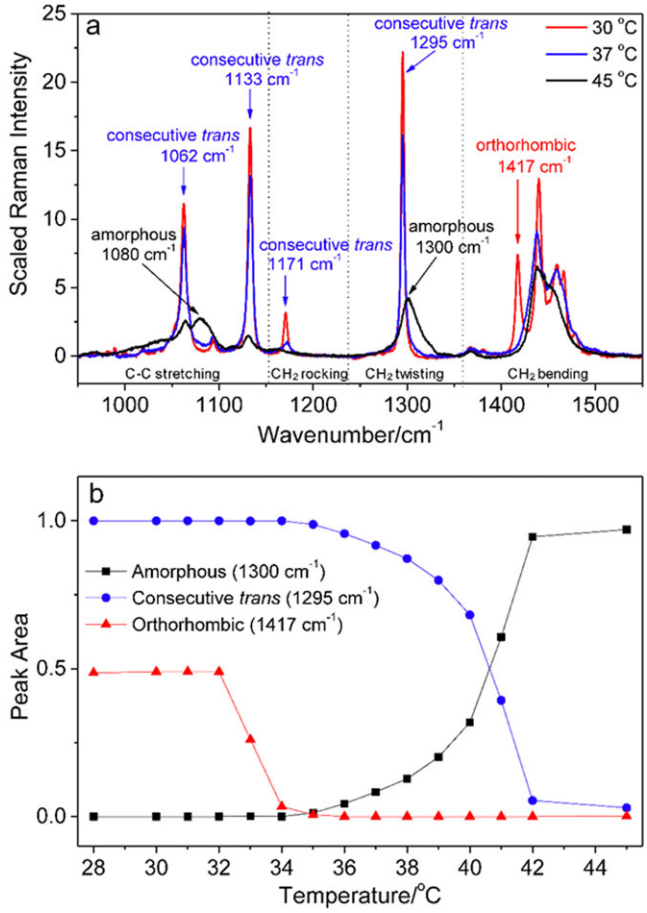

Figure 1. (a) Three representative Raman spectra of *n*-$C_{21}H_{44}$ during melting. All spectra are scaled by the integrated intensity of the CH_2 twisting region between 1240 cm^{-1} and 1350 cm^{-1}. (b) Temperature-dependent peak intensity of three selected Raman bands. The peak intensity of each band is presented as the peak area calculated from fitting the band with a Lorentzian function.

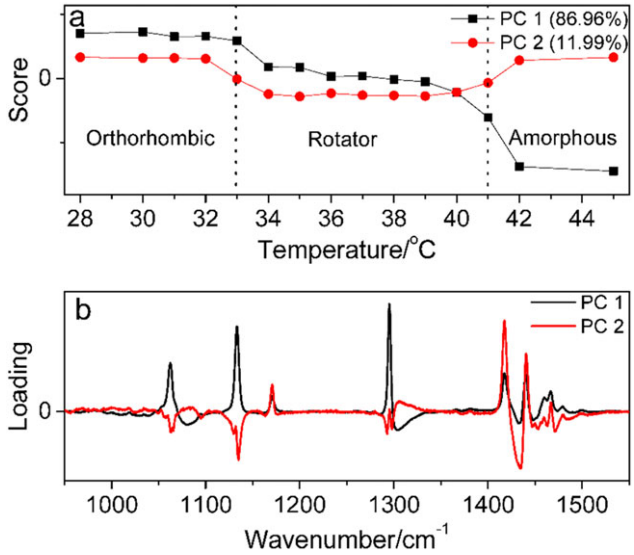

Figure 2. Principal component analysis of the variable temperature Raman spectra of *n*-$C_{21}H_{44}$. (a) Scores of the first two principal components (PC1 and PC2) as a function of temperature, and (b) loading spectra of the two PCs.

Multivariate analysis methods have been widely used to detect subtle changes over the multiple spectral components. Principal component analysis (PCA) is one of the simplest MVA methods that finds orthogonal spectral components (called loadings) and their relative amplitudes (called scores) with the orders of principal components determined from the highest variance. The plot of PCA scores as a function of temperature in Fig. 2a shows two distinctive transition temperatures. As seen in the individual peak intensity plots of Fig. 1b, the transition from the orthorhombic phase to the rotator phase occurs in the same region between 32 °C and 34 °C. It is noted that the PCA score plot resolves the transition from the rotator to the amorphous state in a much narrower range of 39 °C and 42 °C than the range of 34 °C and 42 °C observed in Fig. 1b. Despite the better resolving power of phase transition temperature, a loading spectrum from the PCA shown in Fig. 2b does not correspond to a specific single conformation because it simply represents a linear combination of independent spectra that generates the greatest variance over the perturbation. Therefore, PCA is in general limited in identifying individual Raman modes directly associated with specific molecular conformations.

We use the 2DCOS analysis to obtain both direct spectral correlations with specific perturbation and sufficient sensitivity and resolving power to detect subtle spectral changes and overlapping peaks during phase transitions. The 2DCOS analysis is based on the correlation between pairs of spectral peaks in a series of spectra acquired as a function of an experimental perturbation. Briefly, the synchronous correlation, $\varphi(\nu_1,\nu_2)$, represents directionality of intensity changes of the two frequency components of ν_1 and ν_2. Positive $\varphi(\nu_1,\nu_2)$ indicates that the two components change in the same direction while negative $\varphi(\nu_1,\nu_2)$ indicates the opposite direction. On the other hand, the asynchronous correlation, $\psi(\nu_1,\nu_2)$, represents the sequential order of intensity changes of the ν_1 and the ν_2 components. The sequence can be determined by considering both $\varphi(\nu_1,\nu_2)$ and $\psi(\nu_1,\nu_2)$ according to a general rule, proposed by Noda.[12] When $\varphi(\nu_1,\nu_2)$ and $\psi(\nu_1,\nu_2)$ are the same sign, the ν_1 changes earlier than the ν_2. When $\varphi(\nu_1,\nu_2)$ and $\psi(\nu_1,\nu_2)$ are the opposite sign, the ν_1 changes later than the ν_2. The 2DCOS maps can be useful not only to determine the sequential order of spectral changes but also to enhance spectral resolution by spreading highly overlapped peaks along a second orthogonal dimension.[19,20]

Figure 3 shows the 2D synchronous and asynchronous correlation maps of 13 Raman spectra of *n*-$C_{21}H_{44}$ measured between 30 °C and 42 °C, which covers the rotator phase and parts of orthorhombic and amorphous phases. Among the cross correlation pairs, we examine those between the 1417 cm^{-1} band (from the orthorhombic phase) and six other bands in (1040 to 1200) cm^{-1} and (1050 to 1110) cm^{-1} regions. First, the consecutive *trans* conformation bands at 1062 cm^{-1}, 1133 cm^{-1}, 1170 cm^{-1}, and 1295 cm^{-1}, show positive $\varphi(\nu_1,\nu_2)$, indicating that both the consecutive *trans* and the orthorhombic bands respond to the temperature increase in the same direction. The negative (opposite) signs of $\psi(\nu_1,\nu_2)$ indicate that the orthorhombic band at 1417 cm^{-1} decreases earlier than the consecutive *trans* bands originating from the rotator phase. These correlation results are consistent with the previous observation that the orthorhombic phase proceeds the rotator phase. Next, for the amorphous bands at 1080 cm^{-1} and 1301 cm^{-1}, the negative $\varphi(\nu_1,\nu_2)$ values indicate that the amorphous state bands and the orthorhombic state band respond to the temperature increase in opposite directions. The positive (opposite) $\psi(\nu_1,\nu_2)$ indicate that the amorphous bands increase occurs after the orthorhombic peak decrease. The 2DCOS analysis results can be summarized as:

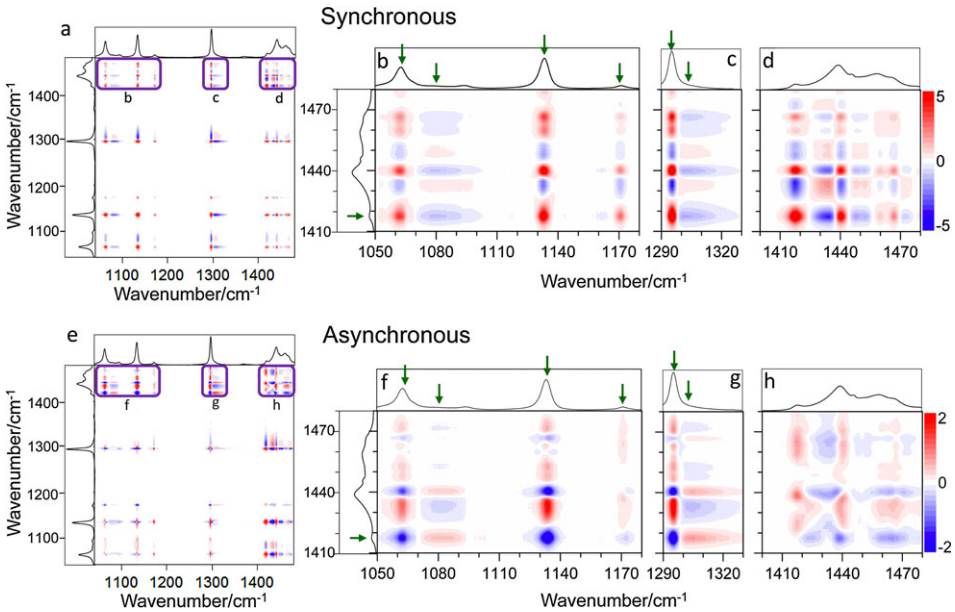

Figure 3. (top) Synchronous and (bottom) asynchronous 2D correlation maps of the *n*-$C_{21}H_{44}$ Raman spectra over a temperature range from 30 °C to 42 °C at 1 °C steps. The red and blue colors denote positive and negative cross peaks, respectively, as indicated by the scale bars on the right. The rectangular boxes in (a) and (e) are enlarged into (b – d) and (f – h), respectively. Pairs of the bands indicated by the green arrows are discussed in the text.

(orthorhombic phase) → (rotator phase) → (amorphous phase), which is consistent with the known individual peak intensity analysis and the PCA results.

The 2DCOS analysis reconfirms the sequence of rise and fall of Raman bands associated with the multiple phases of *n*-$C_{21}H_{44}$. However, performing 2DCOS over the whole temperature range from 30 °C to 42 °C cannot provide phase specific information of Raman bands. As an alternative, the MW-2DCOS partitions the spectra into small temperature windows and analyzes a series of the 2DCOS of the partitioned windows. The window size determines the temperature "resolution" of the analysis as well as the "signal-to-noise ratio" of the 2DCOS results. We find that the minimum window size of three temperature steps ($\Delta T = 2$ °C) still provides signal-to-noise ratio sufficient for the 2DCOS analysis. Figures 4a and 4b show two examples of the synchronous maps from the windows centering at 33 °C and 41 °C, near the phase transition temperatures. The diagonal line is called the autocorrelation spectrum, which corresponds to the total intensity variation within the window range.[12] The moving-window autocorrelation spectra in Fig. 4c and 4d clearly show two distinctive phase transition temperatures, where intensity variation reaches local maxima. The moving-window autocorrelation plots also show which Raman bands are associated with a specific phase transition. The two distinctive transition temperatures of 33 °C and 41 °C correspond to the orthorhombic-to-rotator and rotator-to-amorphous transitions, respectively, as previously discussed in the individual peak analysis and the PCA. The two phase transition temperatures determined by MW-2DCOS are consistent with the previously reported values for *n*-$C_{21}H_{44}$ by X-ray (32.55 °C and 40.55 °C), and differential scanning calorimetry (DSC) (30.84 °C and 40.01 °C).[21,22] Interestingly, the autocorrelation intensity of the consecutive *trans* peaks at 1133 cm^{-1}, 1062 cm^{-1}, and 1295 cm^{-1} shows maxima not only at the rotator-to-amorphous transition (41 °C) but also at the orthorhombic-to-rotator transition (33 °C), which are not observable in the individual peak intensity analysis in Fig. 1a. Existence of the two maxima strongly suggests that the orthorhombic-to-rotator transition affects the consecutive *trans* modes and that MW-2DCOS is sufficiently sensitive to detect these subtle spectral changes.

Next, we analyze the crowded region of CH_2 bending (1410 cm^{-1} to 1480 cm^{-1}) with MW-2DCOS to find whether correlations of the embedded peaks and their association with specific phases can be resolved. During the orthorhombic-to-rotator transition (from 32 °C to 34 °C), as shown in Fig. 5a, the two narrow split peaks at 1417 cm^{-1} and 1440 cm^{-1} distinctly become a single, broad peak at 1437 cm^{-1}. These peak changes appear in the 2DCOS results as the positive cross peak between 1417 cm^{-1} and 1440 cm^{-1} and the negative cross peak between 1417 cm^{-1} and 1437 cm^{-1} in the synchronous map of Fig. 5c. It is noted that the cross peak regions in the asynchronous map of Fig. 5e show weak but non-zero values. The cross peaks in the asynchronous maps during the rotator-to-amorphous transition of Fig. 5f also show weak but non-zero values. These non-zero values in the asynchronous correlation maps can be explained in two ways: (1) the peaks corresponding to one or both of the conformations shift or broaden during the phase transition; and (2) there exists an additional state between the orthorhombic and the rotator phases. However, because this region contains other overlapping Raman modes, including the methylene scissoring mode, the antisymmetric methyl bend mode, and possibly an IR band overtone in Fermi resonance,[23,24] it is challenging to prove which explanation is correct by analyzing these highly overlapping bands. Therefore, we analyze more isolated Raman bands in order to find more conclusive Raman characterization of the phase transitions.

Figure 6 shows the synchronous and asynchronous maps calculated at three moving windows for the consecutive *trans* band at 1295 cm^{-1}. During the orthorhombic-rotator transition (32 °C to 34 °C), both synchronous and asynchronous correlation maps exhibit non-zero values, indicating the consecutive *trans* peak at 1295 cm^{-1} changes in the temperature window. The evolution of qualitative patterns on the 2DCOS maps can be converted into a

Journal of RAMAN SPECTROSCOPY

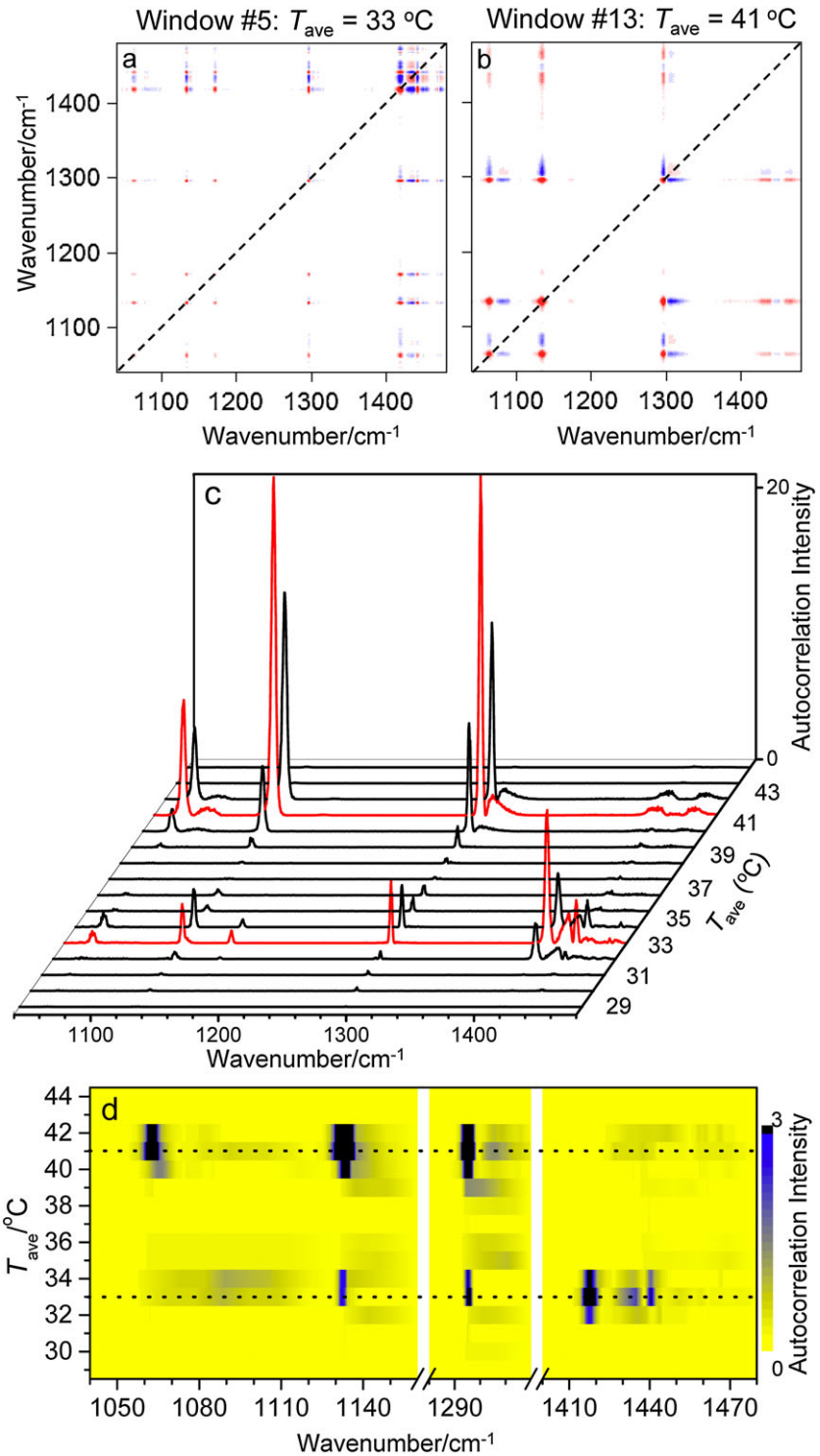

Figure 4. Moving-window two-dimensional correlation spectroscopy (MW-2DCOS) analysis of the *n*-$C_{21}H_{44}$ Raman spectra with a temperature window size of three spectra ($\Delta T = 2$ °C). Examples of synchronous maps are presented for two selected average temperatures (T_{ave}) at (a) 33 °C and (b) 41 °C. (c) The autocorrelation or autopeak spectrum, corresponding to the diagonal line in a synchronous map, is plotted as a function of T_{ave} of the moving window. (d) The identical data of (c) are re-plotted differently for determination of phase transitions over the whole range of Raman bands. The two phase transitions are indicated as the black dotted lines.

metric that allows for comprehensible visualization of the phase transition. Our approach is to measure the correlation intensity of an identical region of both synchronous and asynchronous maps for all temperature windows. We set an isosceles right triangle because it is applicable to both synchronous and asynchronous maps, which are symmetrical and antisymmetrical across the diagonal line, respectively. The width of the triangle is set by the peak width determined from a synchronous map. The average values of synchronous and asynchronous correlation are plotted as a function of the average temperature (T_{ave}) of a temperature window in

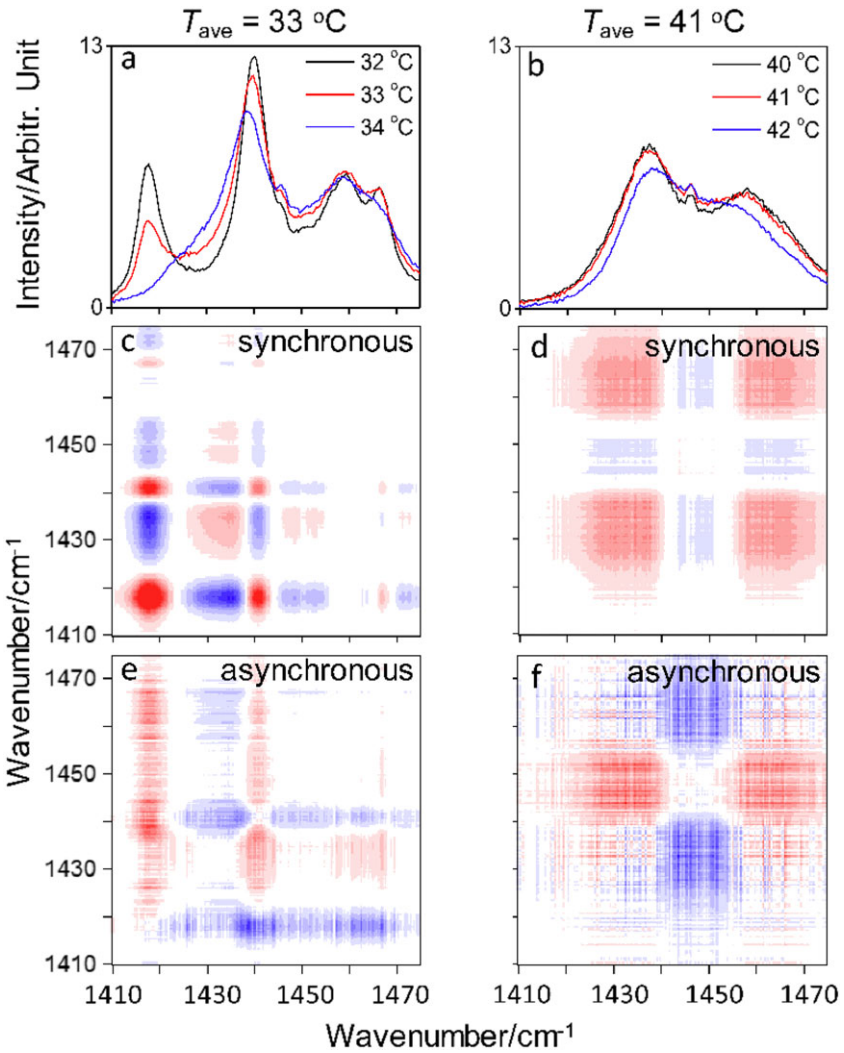

Figure 5. Raman spectra in the CH_2 bending region of *n*-$C_{21}H_{44}$ at two temperature windows corresponding to the orthorhombic-to-rotator transition (T_{ave} = 33 °C; the left column) and the rotator-to-amorphous transition (T_{ave} = 41 °C; the right column). The synchronous (c, d) and asynchronous (e, f) maps are 2DCOS results of the two selected windows.

Fig. 6g and 6h, respectively. This new type of quantitative visualization from MW-2DCOS helps to determine the location of a phase transition, which corresponds to T_{ave} for the maximum in spectral variation. The width of the peak indicates the sharpness of a phase transition. In Fig. 6g and 6h, the full-width-half-maximum (FWHM) is approximately 2 °C, which happens to be the width of the moving window for this analysis, indicating that the transition occurs within a temperature range equal to or narrower than 2 °C.

It needs to be noted that the non-zero asynchronous correlation, as shown in Fig. 6d, cannot be explained with a simple two state model where a spectrum is reduced into a linear combination of the unvarying spectra corresponding to the crystalline and amorphous states. We exclude the possibility of existence of a fourth phase because it is unlikely that there exists a new phase between the orthorhombic phase and the rotator phase and that it only exists between 33 °C and 34 °C. Previous X-ray and DSC studies also do not indicate any additional temporary phase between the orthorhombic and rotator phases. Therefore, we turn to the possibility of band shape changes in one or both of the phases. It is well known that band position shifts and line broadening can cause non-zero asynchronous correlation.[12] We examine the band position and linewidth of the 1295 cm^{-1} band and the two other consecutive *trans* bands of 1062 cm^{-1} and 1133 cm^{-1} by fitting them with a single pseudo-Voigt function (a linear combination of one Gaussian and one Lorentzian function). We find that a pseudo-Voigt function can fit experimental data much better than a single Lorentzian or a single Gaussian function, shown in Fig. S1 (Supporting Information). From the fitting, we determined amplitude, band position, FWHM, and Lorentzian percentage of each band. We include the contribution of a broad amorphous band into the fitting and find that the results of the consecutive *trans* bands below 41 °C are not affected by the broad amorphous band. Figure 7 plots the band position and FWHM of the three peaks as a function of temperature. All three peaks exhibit changes in the temperature dependence of band position and width below and above the phase transition temperature at ≈33 °C. In the orthorhombic phase ($T < 33$ °C), band position and width do not show a measureable temperature dependence. In contrast, in the rotator phase ($T > 33$ °C), it is clear that band position shifts and the width broadens with temperature. In addition, only in the rotator phase, Lorentzian percentage in the pseudo-Voigt function increases with temperature, shown in Fig. S2 (Supporting Information).

Journal of RAMAN SPECTROSCOPY

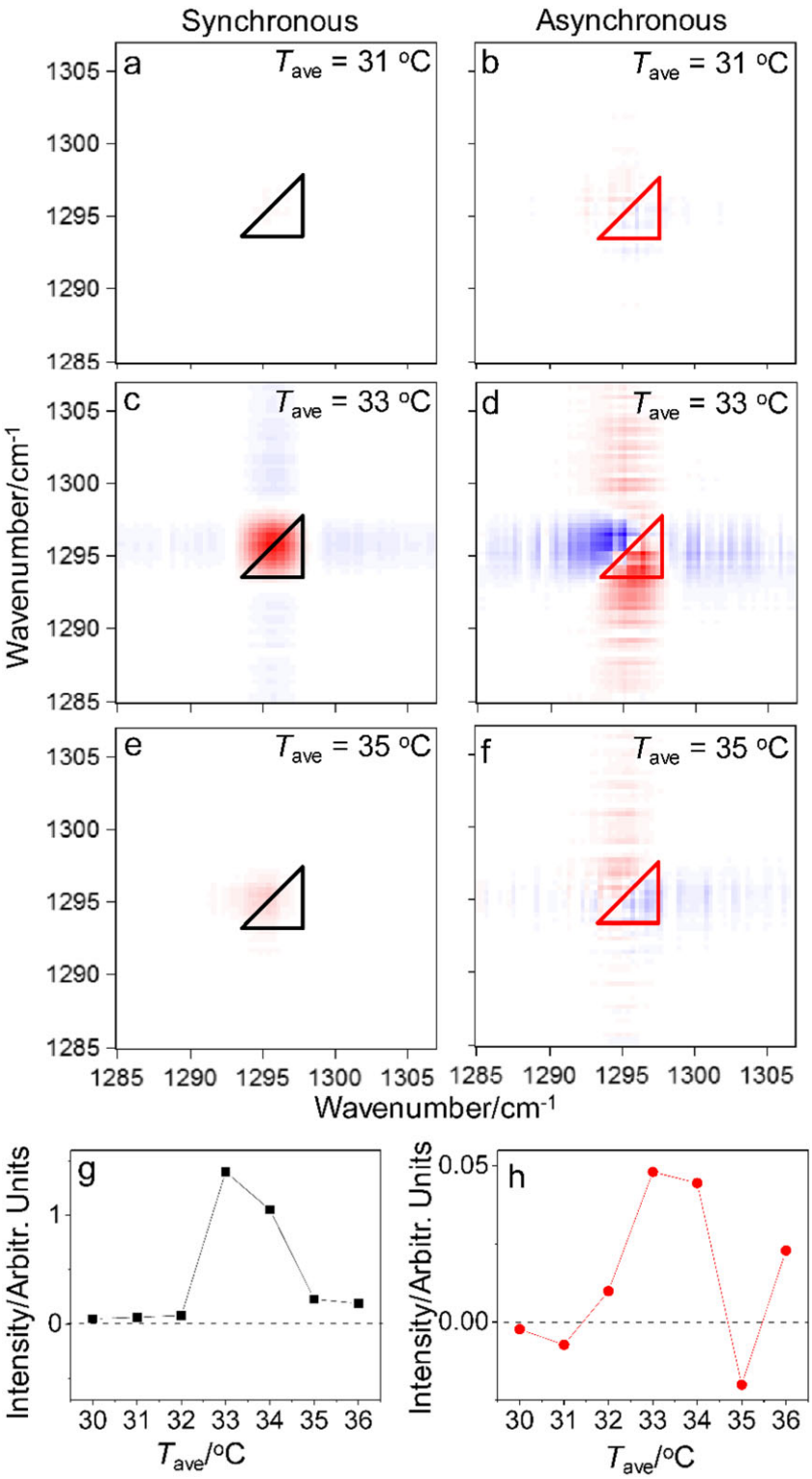

Figure 6. (a) – (f) Synchronous and asynchronous correlation maps of the CH_2 twisting mode of *n*-$C_{21}H_{44}$, peaked at 1295 cm^{-1}, are calculated from temperature windows in the range of the orthorhombic and rotator phases. The intensity scale is from −4.6 0 to 4.6 for the synchronous maps and from −0.2 to 0.2 for the asynchronous maps. An isosceles right triangle is drawn to have the center of the hypotenuse located at the center of the peak in the synchronous map and to have the side length match the width of the peak. The average intensity within the triangle is plotted as a function of T_{ave} for the synchronous (g) and asynchronous (h) maps.

Previous studies based on peak intensity are focused on gradual decrease in consecutive *trans* contribution in the rotator phase with increasing temperature. Orendorff *et al.*[23] analyzed the peak intensities, peak frequencies, and bandwidths of several Raman bands of octadecane and PE, but they assigned the intermediate state as a biphasic mixture where the (orthorhombic) crystalline phase and the (amorphous) liquid phase coexist. Our results of temperature-dependent peak position, width, and shape of the consecutive

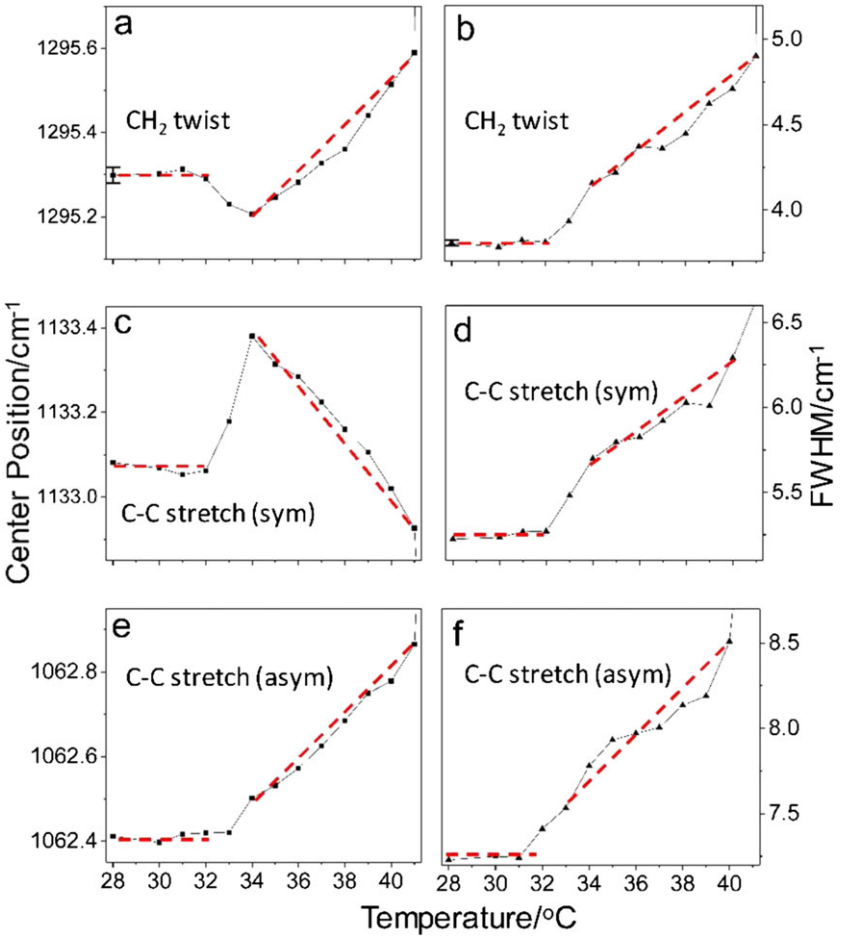

Figure 7. Peak fitting results of three selected consecutive *trans* bands in the temperature range corresponding to the orthorhombic and rotator phases. Peak position and FWHM determined from the fitting with a single pseudo-Voigt function are plotted as a function of temperature in the left and right columns, respectively. The error bars of ±0.018 cm^{-1} in (a) and ±0.017 cm^{-1} in (b) indicate the standard deviations of the peak position and FWHM fitted from three spectra, which were separately acquired at 28 °C. The red dashed lines are for guidance.

trans Raman modes, in Fig. 7, clearly show qualitatively different temperature dependence of peak position and width between the orthorhombic and rotator phases. In particular, the kinks and the offsets at 33 °C in the peak position plot of Fig. 7a and 7c strongly suggest that the rotator phase provides the consecutive *trans* modes with a unique molecular environment that is qualitatively different from the orthorhombic phase. It is known that the unit cell of the rotator phase is hexagonal, which is different from the orthorhombic unit cell of the crystalline phase. It is interesting that the rotator phase exhibits a higher sensitivity to temperature in peak position and width compared to the orthorhombic phase. Orendorff *et al.*[23] ascribed the blue shift of the CH_2 twisting bands of octadecane at 1295 cm^{-1} to a reduced coupling between alkane chains. Interestingly, in the same report, they correlated the bandwidth broadening of the same band with both an increase in rotational disorder and an increase in the number of gauche conformers. Their studies, though, were more focused on conformational differences between the crystalline and the amorphous phases. It remains unclear whether intermolecular chain interaction or intramolecular conformational order causes the unique temperature dependence of the consecutive *trans* bands in the rotator phase. However, it is clear that the molecular environment of the orthorhombic and the rotator phase are qualitatively different and that the trends of peak position, bandwidth, and Lorentzian percentage are monotonic with temperature in the rotator phase.

The temperature-dependent peak shifting and broadening explain the non-zero asynchronous correlation at the orthorhombic-to-rotator phase transition in Fig. 6. By using the empirical trend found by the peak fitting analysis, we construct and compare a few potential Raman band models to unravel the complex feature in the 2DCOS map in Fig. 6d. The first model assumes a single peak in the orthorhombic phase and an independent single peak in the rotator phase. In this model, the spectra at 32 °C and 34 °C are fit to single pseudo-Voigt profiles. The Raman spectrum at 33 °C is expressed as the linear combination of the peak function at 32 °C and the extrapolated peak function from the trend between 34 °C and 40 °C, and their relative amplitudes are determined by fitting with the experimental spectrum at 33 °C. The three spectra simulated from this "single orthorhombic peak" model, depicted in Fig. 8a, generate synchronous and asynchronous maps. The synchronous map from the simulated and experimental spectra looks similar in shape and intensity. However, the asynchronous map is quite different in both intensity and shape between the simulated and experimental results in Fig. 8c and 8i, respectively. Second, we calculated 2D correlation maps for a slightly modified model, which treats the intermediate rotator peak at 33 °C as a single

Journal of RAMAN SPECTROSCOPY

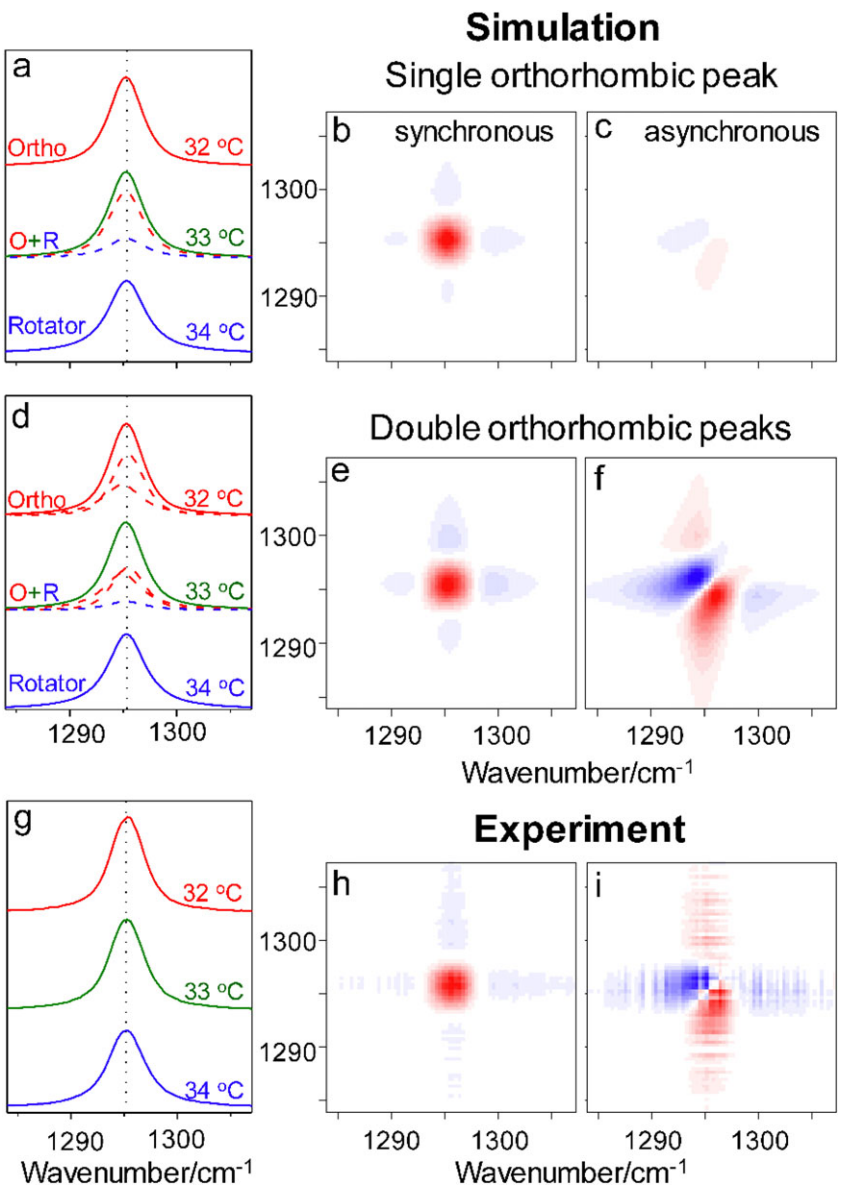

Figure 8. Two examples of Raman band models proposed to explain the 2D correlation maps observed at the orthorhombic-to-rotator transition. The single orthorhombic peak model (a – c) assumes a single peak in the orthorhombic phase while the double orthorhombic peak model (d – f) assumes two overlapping peaks in the orthorhombic phase. In both models, the Raman spectrum at 33 °C, the transition temperature, is assumed to be a mixture of the spectra corresponding to the orthorhombic (O) and the rotator (R) phases. Both synchronous and asynchronous maps calculated from the simulated Raman spectra for 32 °C to 34 °C are compared with the correlation maps obtained from experimental data (g – i). The 2D correlation maps are plotted on the same z scale for comparison: from 0 to 4.2 for the synchronous maps and from 0 to 0.2 for the asynchronous maps. The vertical dotted line at 1295.2 cm^{-1} is for guidance.

pseudo-Voigt function. The generated asynchronous map, shown in Fig. S3 (Supporting Information), is still far from the experimental results.

The third model assumes two overlapping peaks for the orthorhombic spectrum and a single peak for the rotator state. The motivation is that their subtle difference in two molecular configurations in the orthorhombic unit cell can cause splitting in consecutive *trans* Raman bands, as predicted by calculations.[25,26] In this "double orthorhombic peak" model, we fit the orthorhombic band with two peaks, as depicted in Fig. 8d. The rotator peak and the mixture peaks at the transition temperature are prepared in the same way as the first model. Figure 8e and 8f show the 2D correlation maps calculated based on the double orthorhombic peak model. The asynchronous maps from the simulated spectra and the experimental spectra are very similar in both shape and intensity. This similarity suggests that the CH_2 twisting band in the orthorhombic phase theoretical prediction[25,26] and experimental observation at different conditions.[9,11] It must be noted that the consists of resolved by this analysis is 1.4 cm^{-1}, which is extremely challenging for conventional spectral analysis methods to resolve from room-temperature Raman bands with a FWHM of two overlapping peaks, confirming the previous splitting (4 to 6) cm^{-1}. These results demonstrate that MW-2DCOS analysis can determine the orthorhombic-to-rotator phase transition temperature and unravel the overlapping peaks in the orthorhombic state. Figure 9 shows the CH_2 twisting Raman bands at the orthorhombic, rotator, and amorphous phases, accompanied by their schematic structures.

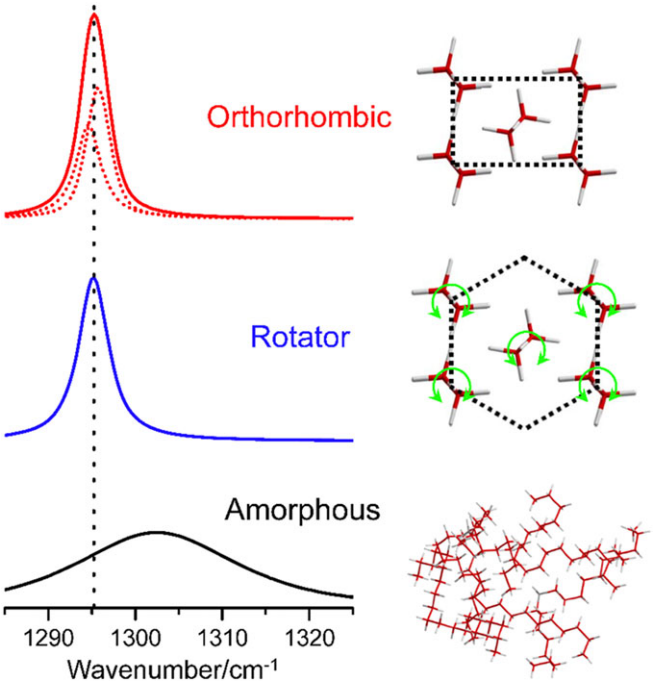

Figure 9. Schematic of spectral evolution of the CH_2 twisting mode of n-$C_{21}H_{44}$ during melting. Two narrow overlapping peaks in the orthorhombic phase becomes a single peak in the rotator phase; then, it becomes broad and shifted to higher frequency in the amorphous phase.

Conclusion

We analyzed a series of variable temperature Raman spectra of n-$C_{21}H_{44}$ during melting from the orthorhombic phase to the rotator phase and to the amorphous phase. We found that MW-2DCOS can determine the orthorhombic-to-rotator and the rotator-to-amorphous transition temperatures with a higher resolving power than the commonly used, individual peak intensity analysis or the principal component analysis. Temperature- and phase-resolved spectral analysis on peak position, bandwidth, and Lorentzian percentage of several Raman bands shows that the intermediate rotator phase is not a simple biphasic mixture of the crystalline and amorphous phases but a unique phase that provides different spectral environment from the other two phases. By comparing with the 2DCOS of the model Raman spectra, we have learned that the CH_2 twisting band at 1295 cm^{-1} consists of two overlapping peaks in the orthorhombic phase but becomes a single peak in the rotator phase, which had been only predicted but not observed because of thermal broadening near the melting temperature. This result demonstrates that MW-2DCOS can be used as a sensitive tool not only for determination of phase transitions but for unraveling subtle spectral features associated a specific molecular conformation.

Acknowledgements

The authors thank Charles Camp from NIST for his valuable comments on the manuscript. Ying Jin acknowledges the support from the NIST Biomanufacturing Program.

Disclaimer

Certain commercial equipment, instruments, or materials are identified in this paper in order to adequately specify the experimental procedure. Such identification does not imply recommendation or endorsement by the National Institute of Standards and Technology, nor does it imply that the materials or equipment identified are necessarily the best available for the purpose.

Official contribution of the National Institute of Standards and Technology; not subject to copyright in the United States.

References

[1] J. F. Nagle, S. Tristram-Nagle, *Curr. Opin. Struc. Biol.* **2000**, *10*, 474.
[2] G. van Meer, D. R. Voelker, G. W. Feigenson, *Nat. Rev. Mol. Cell Bio.* **2008**, *9*, 112.
[3] E. B. Sirota, H. E. King, D. M. Singer, H. H. Shao, *J. Chem. Phys.* **1993**, *98*, 5809.
[4] A. P. Kotula, A. R. Hight Walker, K. B. Migler, *Soft Matter* **2016**, *22*, 5002.
[5] P. K. Mukherjee, *Rsc. Adv.* **2015**, *5*, 12168.
[6] A. Tarazona, E. Koglin, B. B. Coussens, R. J. Meier, *Vib. Spectrosc.* **1997**, *14*, 159.
[7] G. R. Strobl, W. Hagedorn, *J. Polym. Sci. Pol. Phys.* **1978**, *16*, 1181.
[8] K. B. Migler, A. P. Kotula, A. R. H. Walker, *Macromolecules* **2015**, *48*, 4555.
[9] F. J. Boerio, J. L. Koenig, *J. Chem. Phys.* **1970**, *52*, 3425.
[10] R. G. Snyder, *J. Mol. Spectrosc.* **1961**, *7*, 116.
[11] M. Kobayashi, H. Tadokoro, R. S. Porter, *J. Chem. Phys.* **1980**, *73*, 3635.
[12] I. Noda, Y. Ozaki, *Two-Dimensional Correlation Spectroscopy: Applications in Vibrational and Optical Spectroscopy*, vol. *61*, Wiley, Chichester, UK, **2004**.
[13] Y. Jin, W. Wang, Z. H. Su, *Macromolecules* **2011**, *44*, 2132.
[14] Y. Jin, W. Wang, Z. H. Su, *Polym. Chem-Uk* **2012**, *3*, 2430.
[15] S. Morita, H. Shinzawa, I. Noda, Y. Ozaki, *J. Mol. Struct.* **2006**, *799*, 16.
[16] B. J. Sun, Q. Jin, L. S. Tan, P. Y. Wu, F. Yan, *J. Phys. Chem. B* **2008**, *112*, 14251.
[17] M. Thomas, H. H. Richardson, *Vib. Spectrosc.* **2000**, *24*, 137.
[18] T. Zhou, A. Zhang, C. S. Zhao, H. W. Liang, Z. Y. Wu, J. K. Xia, *Macromolecules* **2007**, *40*, 9009.
[19] Y. Ozaki, I. Noda, J. Near Infrared, *Spec.* **1996**, *4*, 85.
[20] L. Ma, V. Sikirzhytski, Z. M. Hong, I. K. Lednev, S. A. Asher, *Appl. Spectrosc.* **2013**, *67*, 283.
[21] V. Chevallier, M. Bouroukba, D. Petitjean, D. Barth, P. Dupuis, M. Dirand, *J. Chem. Eng. Data* **2001**, *46*, 1114.
[22] J. Doucet, I. Denicolo, A. Craievich, *J. Chem. Phys.* **1981**, *75*, 1523.
[23] C. J. Orendorff, M. W. Ducey, J. E. Pemberton, *J. Phys. Chem. A* **2002**, *106*, 6991.
[24] D. I. Bower, W. F. Maddams, *The Vibrational Spectroscopy of Polymers*, Cambridge University Press, Cambridge, UK, **1989**.
[25] H. W. Li, H. L. Strauss, R. G. Snyder, *J. Phys. Chem. A* **2004**, *108*, 6629.
[26] M. Tasumi, T. Shimanouchi, *J. Chem. Phys.* **1965**, *43*, 1245.

Supporting information

Additional supporting information may be found in the online version of this article at the publisher's web site.